WFPS-TME-059

SEPTEMBER 30, 1977

THERMAL DESIGN AND ANALYSIS OF SUPERCONDUCTORS FOR THE TOROIDAL FIELD COILS OF TNS

fusion power systems department

Westinghouse Electric Corporation

P.O. Box 10864, Pgh. Pa. 15236

DISCLAIMER

WFPS-TME-059
SEPTEMBER 30, 1977

THERMAL DESIGN AND ANALYSIS OF SUPERCONDUCTORS FOR THE TOROIDAL FIELD COILS OF TNS

A. Y. LEE

PREPRINT OF A PAPER TO BE PRESENTED AT THE
SEVENTH SYMPOSIUM ON ENGINEERING PROBLEMS OF FUSION RESEARCH
KNOXVILLE, TENNESSEE, OCTOBER 25-28, 1977

fusion power systems department

Westinghouse Electric Corporation
P.O. Box 10864, Pgh. Pa. 15236

ACKNOWLEDGEMENT

This work was performed for the Oak Ridge National Laboratory Fusion Energy Division, under U.S. Energy Research and Development Administration Contract W-7405-ENG-26, Subcontract 7117. Reproduction, translation, publication, use and disposal, in whole or in part, by or for the United States Government is permitted.

LEGAL NOTICE

FOREWORD

The Division of Magnetic Fusion Energy within the U.S. Energy Research and Development Administration has initiated within the fusion development program for tokamak power reactors a series of systems studies aimed at the definition of subsequent generations of tokamak devices leading to a commercial prototype reactor. Since April, 1976, a design team composed of representatives from the ORNL Fusion Energy Division and the Westinghouse Fusion Power Systems Department has been engaged in scoping studies associated with the definition of The Next Step (TNS) in the tokamak program after the TFTR. Provisional goals established for TNS include:

- achievement of ignition
- demonstration of burning dynamics
- evaluation of design requirements and solutions for long pulse operation
- features which extrapolate to a viable power reactor
- availability in the mid-to-late 1980's

It is in this context that the work reported herein was performed.

THERMAL DESIGN AND ANALYSIS OF SUPERCONDUCTORS FOR THE TOROIDAL FIELD COILS OF TNS

Abstract

The toroidal field coils in two of the four TNS field coil design options are superconducting. NbTi superconductors are used in the low field design option and Nb_3Sn superconductors are used in the high field design option. The preliminary conceptual design parameters of the coils and the superconductors have been developed. The selected coil shape is the pure tension D-configuration. The superconductors are the multifilamentary, cabled design and are cooled by forced flow supercritical helium. Thermal stability analyses were performed for the superconductors. The cryogenic recovery capability of the NbTi superconductors is more than 10^5 J/m^3 of conductor plus helium volume and that of the Nb_3Sn is more than 3×10^5 J/m^3.

Introduction

The Next Step (TNS) ignition tokamak is currently being studied with four toroidal field coil design options. The four options are: (1) TNS-1 with water cooled copper coils; (2) TNS-3 with NbTi superconducting coils; (3) TNS-4 with Nb_3Sn superconducting coils and (4) TNS-5 with hybrid water cooled and NbTi superconducting coils. The merits, costs, risks and technology development requirements for each design option to achieve the ignition test reactor objectives are discussed in References (1) and (2). The superconducting coils require new technology developments and laboratory demonstrations. The thermal design of these coils to meet stability requirements are of interest to coil designers. The thermal analysis of the superconducting coils is the subject of this paper.

The selection of reference parameters for thermal analyses was made on the basis of an early scoping point design, prior to the development of the final design point selections described in Reference (1). The early design point chosen is considered representative and was used as the basis for the development of component models for the overall tokamak system as described in Reference (3).

The primary objective of the thermal design of the superconducting coils is that the superconductors satisfy the cryostability requirement. The present stability requirement specifies that the superconductor shall be able to recover to its fully superconducting state, after an event in which an amount of heat of 10^5 J/m^3 conductor plus helium volume is suddenly deposited in the conductor along a maximum of one half of a turn of the conductor winding, driving that length of the conductor to a normal resistive state. The superconductors and the cooling system are, therefore, to be designed to meet this criterion. The design parameters of the two superconductor options are described and the results of the stability analysis are presented in the following sections of this paper.

Coil Shape and Superconductor Design Parameters

Based on the toroidal field coils design studies for the EPR[4,5] for Dee and oval shape coils, the TF coils for the TNS are selected to be the pure tension Dee shape design with trapezoidal cross section. The inner legs of the coils are wedged against a bucking cylinder to resist the centering force. The central ohmic heating coils are located inside the bucking cylinder and are enclosed by an inner common dewar. The outer portion of each coil is enclosed by a separate dewar. The individual outer dewars mate with the central dewar outside the vertical legs of the coils. Because of the significant influence of size of the ohmic heating coils on the cost of the OH power conversion system and the 1/R dependence of the magnetic field, the optimum major radius of the device was determined to be about 5 m. The overall dimensions of the reference NbTi and Nb_3Sn coils selected for this analysis are listed in Table 1. The algorithms for determining the device cost as a function of size are discussed in detail in Reference (3).

For the superconductors a multifilamentary and cabled design was selected. Copper is used as the stabilizing matrix. The cables are encapsulated by a thin stainless steel jacket. The conductors are cooled by forced flow supercritical helium through the interstices of the strands. The conductors are pancake-wound around the

stainless steel coil support bobbins. These types of superconductor design and cooling method have been shown to be viable for large scale magnetic coils in various analyses and experiments. References (6) and (7) are two examples. The cabled design provides a large heat transfer surface area to strand volume ratio to enhance heat transfer. Forced flow cooling provides flexible control of coolant flow rate to assure cryogenic stability, in spite of the added power requirement for coolant pump work. The major design parameters of the superconductors are shown in Table 2.

The cross sections of the two superconducting coil options are shown in Figure 1. Multiple conductors are wound in parallel along the spiral slot in a bobbin, but are in series to those in the next bobbin. As shown in the figure for the TNS-3 there are five slots in a bobbin with four NbTi superconductors in a slot. The conductors are not graded radially. For TNS-4 there are eight slots in a bobbin with three Nb_3Sn superconductors in a slot. The conductors are graded into 3 radial zones to reduce the cost of superconductors. The conductors in the same slot are to be cooled by a system of parallel hydraulic channels. The coolant would enter the parallel channels near the innermost turn of the coil where the magnetic field is the highest and exit at the outermost turn to a common plenum. One difficulty in this type of parallel channel cooling would arise when one conductor within a parallel flow system is driven to a normal state while the others in the same system remain superconducting. The transition from superconducting to normal increases the resistance to the coolant flow to the faulted channel. The total system coolant flow will be redistributed with the faulted channel receiving less than the design flow and the others receiving more coolant flow. The cryostability analysis to determine the coolant channel inlet flow rate in order to meet the stability requirement should therefore be performed based on a parallel channel fluid flow analysis. The stability analysis method is to be discussed in the following section.

Stability Analysis

For superconducting TF coils the superconductor and the cooling system are designed to be cryostable. The cryogenic recovery capability of a given conductor design is defined as: from what initially imposed normal zone temperature (driven to that

temperature by a sudden heat deposition in the conductor) and normal zone length the conductor can recover to its fully superconducting state. As mentioned previously the stability analysis should include the hydrodynamics of the channel flow in a parallel flow system. The method of solution consists of a coupled heat conduction and fluid flow calculation solving the following equations.

1. Heat conduction in the conductor composite:

$$\nabla(k \nabla T) = \rho C_p \frac{dT}{d\theta} - Q''' \tag{1}$$

$$k \frac{\partial T}{\partial n} = hA_s (T - T_b) \qquad @ \text{ channel wall} \tag{2}$$

where n is the outward normal to the boundary at the channel wall.

2. Axial fluid flow in the cooling channel:

$$\frac{\partial G}{\partial x} + \frac{\partial \rho}{\partial \theta} = 0 \tag{3}$$

$$\frac{\partial (GH)}{\partial x} + \frac{\partial (\rho H)}{\partial \theta} - \frac{1}{J} \frac{\partial p}{\partial \theta} - \frac{QP}{A} = 0 \tag{4}$$

$$\frac{\partial p}{\partial x} + \frac{1}{g} \frac{\partial G}{\partial \theta} + \frac{1}{g} \frac{\partial (G^2 v)}{\partial x} + \tau = 0 \tag{5}$$

where τ = frictional term = $\frac{2f G^2 v}{gD}$ and the other symbols in the equations are defined in the notation section. In addition, the equation of state for the helium is required to determine the fluid properties. For this purpose the NBS helium thermophysical properties data and computer subroutines[8] were used in the analysis. The above equations are solved by a finite difference procedure in a large scale computer.

Temperature dependent thermal properites for the conductor materials and current sharing between the superconductor and the copper substrate are also included in the analysis. In Equation (1) the heat generation term Q''' includes all

components due to nuclear heating, ac losses, joint losses and Joule heating. The Joule heating is the most important component in recovery analysis. The resistive heating depends on the fraction of the transport current in the copper substrate as shown below:

$$Q'''_{I^2R} = \frac{I\, I_{cu}\, \rho_{cu}}{f_c\, A^2_c} \tag{6}$$

where

$$I_{cu} = I, \quad \text{when } T \geq T_{cr} \tag{7}$$

$$I_{cu} = I\left(\frac{T - T_{cs}}{T_{cr} - T_{cs}}\right), \quad \text{where } T_{cs} < T < T_{cr} \tag{8}$$

$$I_{cu} = 0, \quad \text{when } T \leq T_{cs} \tag{9}$$

where

T_{cr} = recovery temperature at a given magnetic field at zero current

T_{cs} = the threshold temperature at which current sharing begins at a given magnetic field and superconductor operating current density

For the NbTi coils with a channel inlet coolant temperature of 4 K and a superconductor operating current density of 25 kA/cm^2, at the peak field location (channel inlet) T_{cr} = 5.6 K and T_{cs} = 4.9 K. For the Nb_3Sn coils with a channel inlet coolant temperature of 5 K, at the peak field zone where the magnetic field is 12 Tesla and the superconductor operating current density is 65.2 kA/cm^2, T_{cr} = 7.5 K and T_{cs} = 6.5 K. At the other two zones these two temperatures are considerably higher. Considering a linear variation of magnetic field from 8 Tesla at the channel inlet to zero at the channel outlet for TNS-3 and similarly, from 12 Tesla to zero for TNS-4, the T_{cr} and T_{cs} temperature profiles along the conductor channels for the two coil options are shown in Figure 2. The area between the T_{cr} and T_{cs} curves is the current sharing region.

In a parallel flow system the channel pressure drop is governed by the system inlet and outlet plenum pressures. A way to simulate the parallel flow analysis is to model one conductor only. The flow boundary conditions specified in the calculation are the channel inlet and outlet pressures (channel Δp) and coolant inlet temperature. When heat is being added to the channel during the recovery transient, the channel inlet flow rate required to satisfy the channel Δp can be determined. At a given initial channel inlet flow rate, if the conductor can recover from an assumed initially imposed normal zone temperature and normal zone length, another higher initial normal temperature is tried until it will not recover. This maximum recoverable initial normal temperature represents the recovery capability of the conductor at the given initial inlet flow rate.

The calculation procedure is first to determine the channel pressure drops of a given conductor design at various channel inlet flow rates under normal operating conditions (all conductors are superconducting). An example of the operating map at normal operating conditions for the NbTi superconductors is shown in Figure 3. In this figure the pumping power required per channel is plotted as a function of channel inlet flow rate for three different cabling combinations. The slanted straight lines are the channel inlet pressures required for a channel length of 120 m to have an exit pressure of 3 atm. This graph also serves the purpose of comparing the pumping power of the different cabling combinations. The 3 x 7 x 7 strand combination was selected for the NbTi superconductors. The channal ΔP at a given inlet flow rate is therefore, obtained from this graph and inputted to the recovery calculation. For example, to determine the recovery capability at an initial channel inlet flow rate of 11 g/s for the NbTi superconductors, a channel inlet pressure of 4.5 atm and outlet pressure of 3 atm together with the coolant inlet temperature of 4 K are specified as the flow boundary conditions in the calculation. In the computations the following major conservative assumptions were made: (1) the channel pressure drop friction factor was based on Hoenig's experimental data on triplex cables[9]; (2) the heat transfer coefficient on the channel wall was evaluated using Giarratano's correlation on smooth tube[10] and (3) the pump efficiency was assumed to be 50% in calculating the refrigeration pumping work. The details of the method of solution are described in Reference (11).

The results of a sample calculation for the NbTi conductor design with an initial coolant inlet flow rate of 11 g/s are shown in Figure 4. The calculated peak conductor temperature and the coolant temperature profiles during the recovery transient, after the conductor was driven normal to 15.5 K, are shown in the figure. Two cases of anlaysis are shown. The solid curves show the case in which one half turn of the conductor winding was driven to 15.5 K initially and the dashed curves show the other case in which the entire conductor length was driven to 15.5 K initially. The calculated coolant inlet flow reductions due to the heat additions during the transient are also shown in the figure. When only one half turn is driven normal, the heat addition is small. The inlet flow reduction amounts to 2.3%. The conductor recovers at about 50 ms. On the other hand, when the entire conductor is driven normal to the same initial normal temperature the heat addition is large. The maximum inlet flow reduction amounts to 12%. The conductor did not recover. This indicates that the hydrodynamics of the fluid flow is quite important and should be included in the recovery analysis.

By the method described above, the recovery capabilities of the NbTi and Nb_3Sn superconductor designs for the TNS-3 and TNS-4 were determined and shown in Figure 5. In this figure the initial heat deposition in J/m^3 of conductor plus helium volume was plotted as a function of the channel initial inlet mass velocity instead of the maximum initial normal zone temperature. It is also noted that the recovery capabilities shown in this figure are for the case when only one half turn of the winding was assumed to be driven to normal initially. This is one of the design ground rules assumed for the design of TNS superconductors.

Because of the greater thermal margin of the Nb_3Sn superconductor, the recovery capability of the Nb_3Sn coils for TNS-4 is much greater and the required coolant flow is much smaller than the NbTi coils for TNS-3. The ideal pumping power requirements at the various channel inlet flow rates are shown in Figure 6. The design points for the two superconducting options are shown by the circles in the two figures.

Summary

Preliminary conceptual designs for the two representative NbTi and Nb_3Sn superconducting TF coil options for the TNS Tokamak have been performed. Cryogenic stability analysis results show that the superconductors have thermal stability margin more than the required value of 10^5 J/m^3 of conductor plus helium volume, after one half of a turn of the winding is driven to a normal state. The physical parameters for each of the two options selected represent a feasible design rather than an optimized one. Once a reference configuration is determined by the cost and performance studies, detailed optimizations can be performed to arrive at a reference design which meets the thermal, structural and magnetic design requirements.

Notation

A	=	channel flow area
A_c	=	cross sectional area of conductor
A_s	=	heat transfer surface area
C_p	=	specific heat at constant pressure
D	=	hydraulic diameter
f	=	fanning friction factor
f_c	=	fraction of copper in the composite
G	=	flow rate per unit area
g	=	gravitational constant
H	=	enthalpy
h	=	heat transfer film coefficient
I	=	conductor transport current
I_{cu}	=	current portion in the substrate
J	=	work-energy conversion factor
k	=	thermal conductivity

P = channel wetted perimeter

p = pressure

Q = heat flux

Q''' = volumetric heat generation rate

T = conductor temperature

T_b = fluid bulk temperature

T_{cr} = superconductor critical temperature at zero transport current

T_{cs} = threshold temperature at which current sharing begins

v = specific volume

x,y,z = Cartesian coordinates

ρ = density

ρ_{cu} = electrical resistivity of substrate (copper)

θ = time

∇ = $\frac{\partial}{\partial x} + \frac{\partial}{\partial y} + \frac{\partial}{\partial z}$

References

1. T. C. Varljen, G. Gibson, J. W. French, and F. M. Heck, "Engineering Parameters For Four Ignition TNS Tokamak Reactor Systems," Paper to be presented at the Seventh Symposium on Engineering Problems of Fusion Research, Knoxville, Tennessee, October 25-28, 1977.

2. D. L. Chapin, H. J. Garber, and G. Gibson, "Trade Study Anslysis For TNS Tokamaks," Paper to be presented at the Seventh Symposium on Engineering Problems of Fusion Research, Knoxville, Tennessee, October 25-28, 1977.

3. D. A. Sink and E. M. Iwinski, "A Computer Code For the Costing and Sizing of TNS Tokamaks," Paper to be presented at the Seventh Symposium on Engineering Problems of Fusion Research, Knoxville, Tennessee, October 25-28, 1977.

4. W. M. Stacey, et al., "Tokamak Experimental Power Reactor Conceptual Design," ANL/CTR-76-3, Argonne National Laboratory, August 1976.

5. M. Roberts, et al., "Oak Ridge Tokamak Experimental Power Reactor Study - 1976, Part 3," ORNL/TM 5574, Oak Ridge National Laboratory, April 1977.

6. V. Arp, "Forced Flow Single-Phase Helium Cooling Systems," Adv. in Cryogenic Engineering, Vol. 17, p. 342, 1972.

7. M. O. Hoenig, et al., "Cryostabilized Single-Phase Helium Cooled Cabled Conductors for Large High Field Superconducting Magnets," Proc. 6th Symposium on Engineering Problems on Fusion Research, p. 586, 1976.

8. R. D. McCarty, "Thermophysical Properties of Helium-4 from 2 to 1500 K with Pressures to 1000 Atmospheres," NBS Tech. Note No. 631, November 1972.

9. M. O. Hoenig, et al., "Supercritical Helium Cooled, Cabled, Superconducting Hollow Conductors for Large High Field Magnets," Proc. 6th International Cryogenic Engineering Conference, p. 310, 1977.

10. P. J. Giarratano, V. D. Arp and R. V. Smith, "Forced Convection Heat Transfer To Supercritical Helium," Cryogenics, Vol. 11, p. 385, 1971.

11. A. Y. Lee, "Cryogenic Recovery Analysis of Forced Flow Supercritical Helium Cooled Superconductors," WFPS-TME-039, Westinghouse Fusion Power Systems Department, August, 1977.

TABLE 1

MAJOR DESIGN PARAMETERS OF THE NbTi AND Nb_3Sn TF COIL OPTIONS FOR TNS
(VALUES SELECTED FOR THERMAL ANALYSIS)

	TNS-3 (NbTi)	TNS-4 (Nb_3Sn)
Major Radius, R_o, m	5.50	4.75
Minor Radius, a, m	1.2	1.0
Peak Field at Winding, B_m, T	8.3	11.6
Field at Axis, B_t, T	4.3	5.8
No. of Coils	20	20
Horizontal Bore, m	5.2	4.9
Vertical Bore, m	7.4	7.8
Mean Coil Circumference, m	22.8	23.8
Outer Radius of Vertical Leg, m	3.1	2.6
Radial Build of Coil, m	0.63	0.82
Coil Cross Sectional Area, m^2	10.8	11.6
Volume of Conductor, m^3	98.9	100.3
Volume of Structure, m^3	117.7	216.6
Stored Energy, MJ	8901.1	14341.3

TABLE 2

MAJOR DESIGN PARAMETERS OF THE NbTi AND Nb_3Sn SUPERCONDUCTORS FOR THE TNS-3 AND TNS-4 COIL OPTIONS (VALUES SELECTED FOR THERMAL ANALYSIS)

	TNS-3 (NbTi)	TNS-4 (Nb_3Sn) Zones		
		1	2	3
Nominal Peak Field, T	8.0	12.0	9.8	7.0
Overall Average Current Density, x 10^7 A/m^2	2.86	2.85	3.75	4.65
S/C Operating Current Density, x 10^9 A/m^2	0.25	0.65	1.25	2.40
Conductor Plus He Area, x 10^{-4} m^2	3.72	5.26	4.0	3.23
Superconductor Area, x 10^{-4} m^2	0.4	0.23	0.12	0.0625
Void Fraction	0.4	0.3	0.35	0.4
Cu:Bronze:Nb_3Sn Ratio	4.6:1(1)	12:3:1	17.7:3:1	27:3:1
Strand Configuration	3 x 7 x 7		3 x 7 x 19	
Strand Diameter, mm	1.39	1.084	0.911	0.786
Wetted Perimeter, m	0.524	0.947	0.859	0.793
Percent Compactness	20	30	25	20
Hydraulic Diameter, mm	1.14	0.67	0.65	0.65
Nominal Channel Length, m	120	45	50	102
Coolant Inlet Temperature, K	4		5	
Approximate Total No. of Parallel Channels	2280		1233	
Estimated Refrigeration Load(2)	88 @ 4 K		38 @ 5 K	

NOTE: (1) Value indicates copper-to-NbTi ratio for TNS-3

(2) Includes pumping power with 50% efficiency, nuclear heating, ac losses and heat leakages.

	TNS-3 (NbTi)	TNS-4 (Nb_3Sn)
Total MA - T	118.5	137.4
I, kA	10	15
Conductor/Coil	292.4	457.9
Bobbin/Coil	29.6	19.1
Slots/Bobbin	5	8
Conductor/Slot	4	3
Structural/SC Area Ratio	1.19	2.16

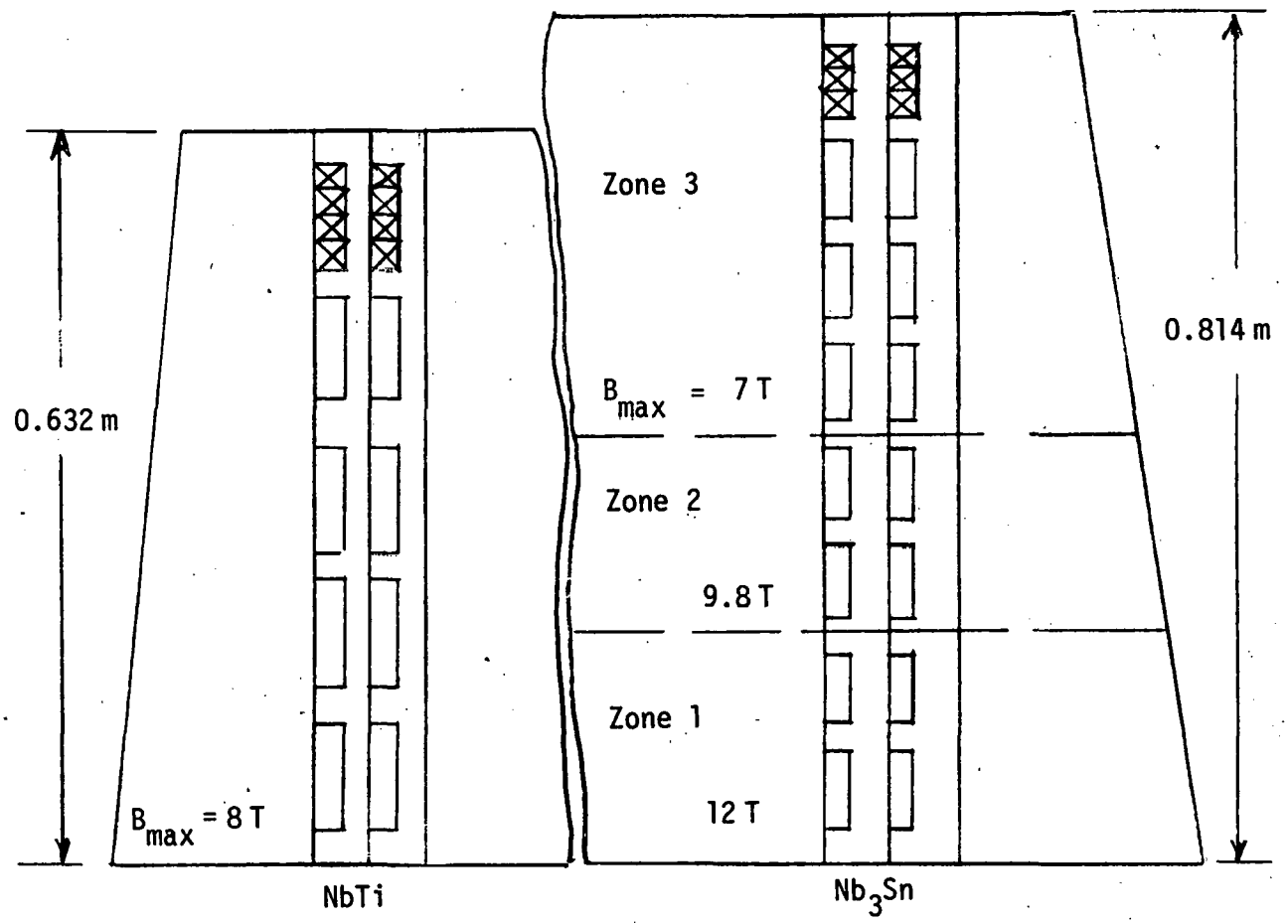

Figure 1. Pancake-Wound TF Coil Cross Sections of TNS-3 and TNS-4

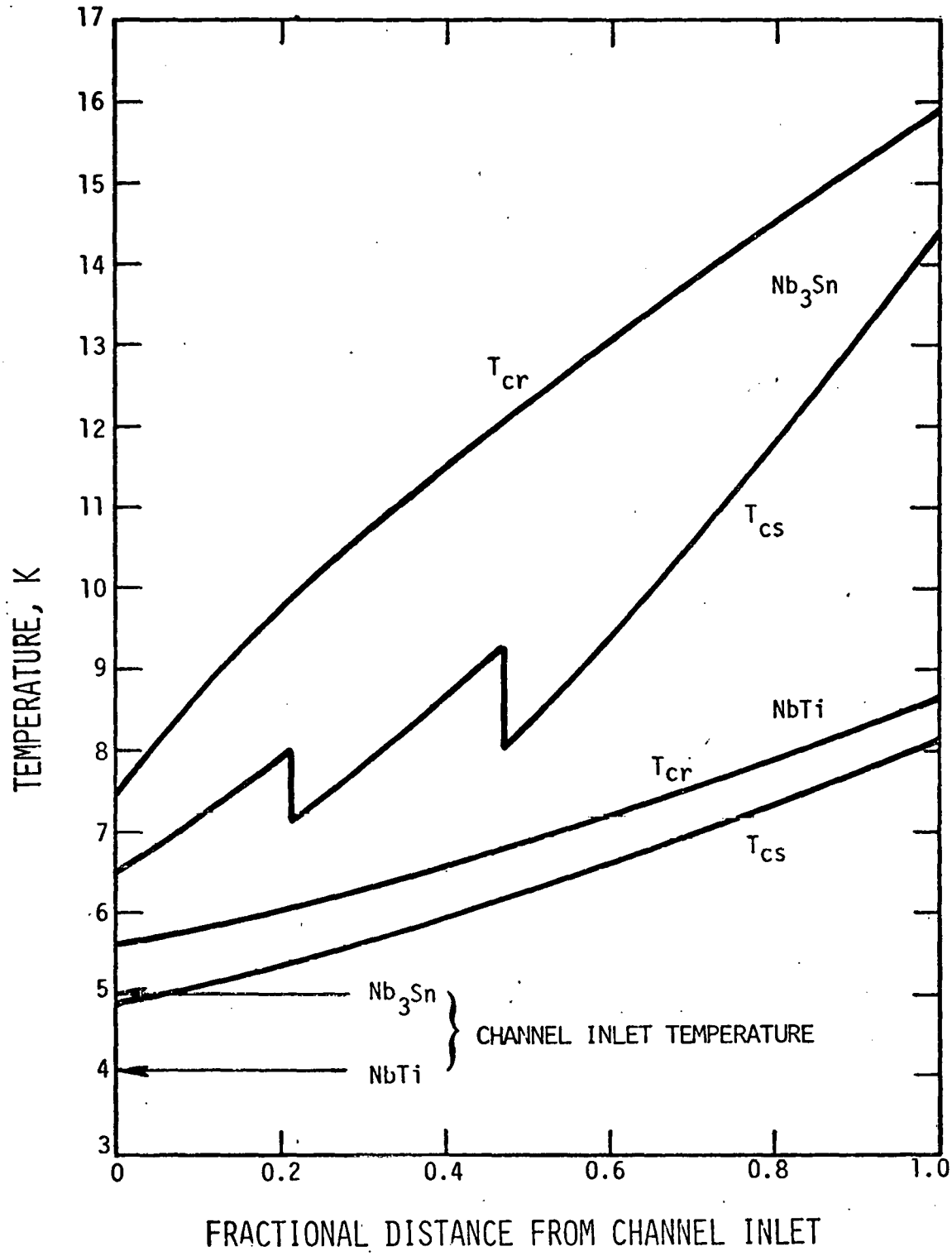

Figure 2. Critical (T_{cr}) and Current Sharing Threshold (T_{cs}) Temperature Profiles for TNS-3 and TNS-4.

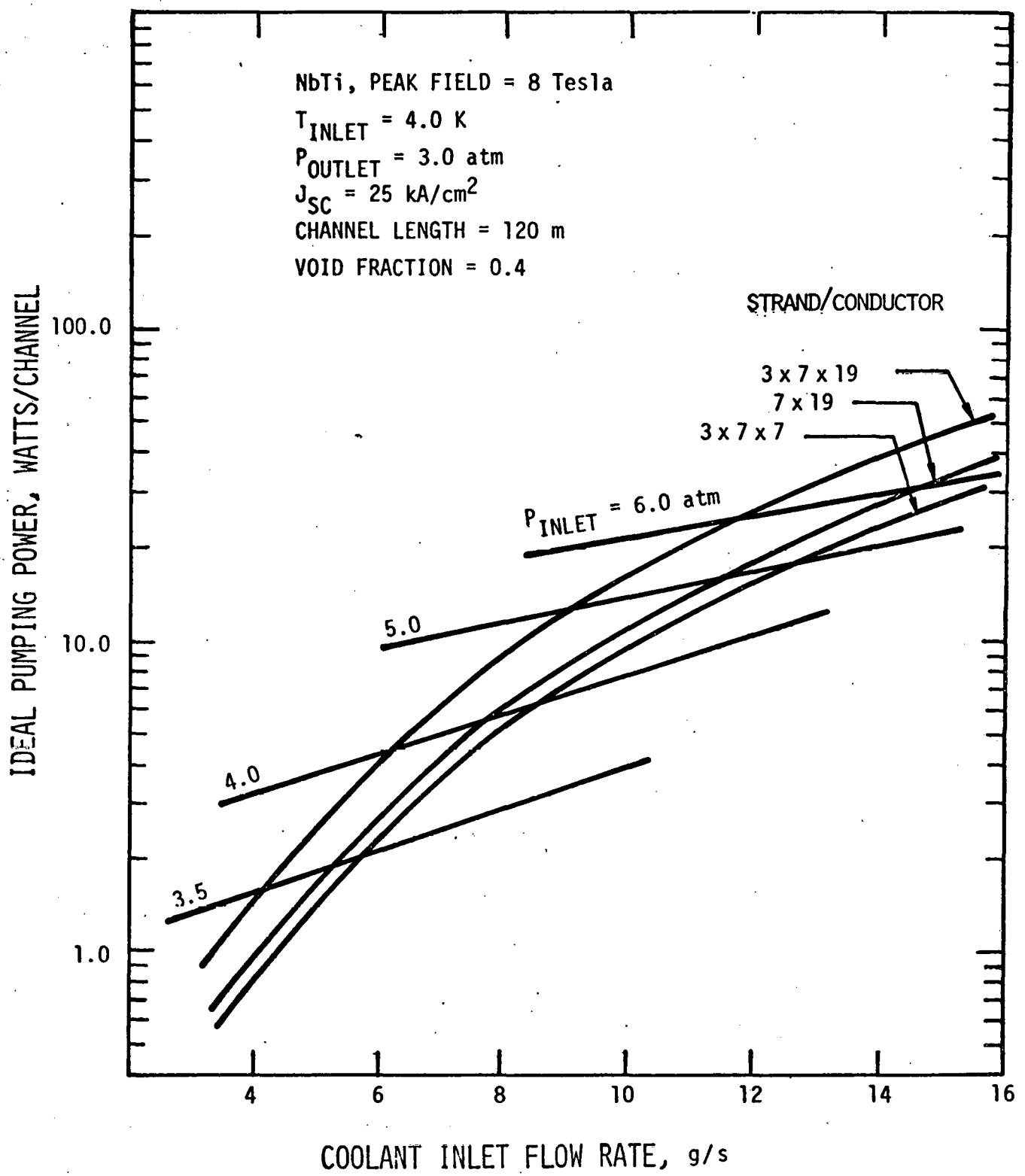

Figure 3. Operating Map of NbTi Superconductors at Normal Operating Conditions.

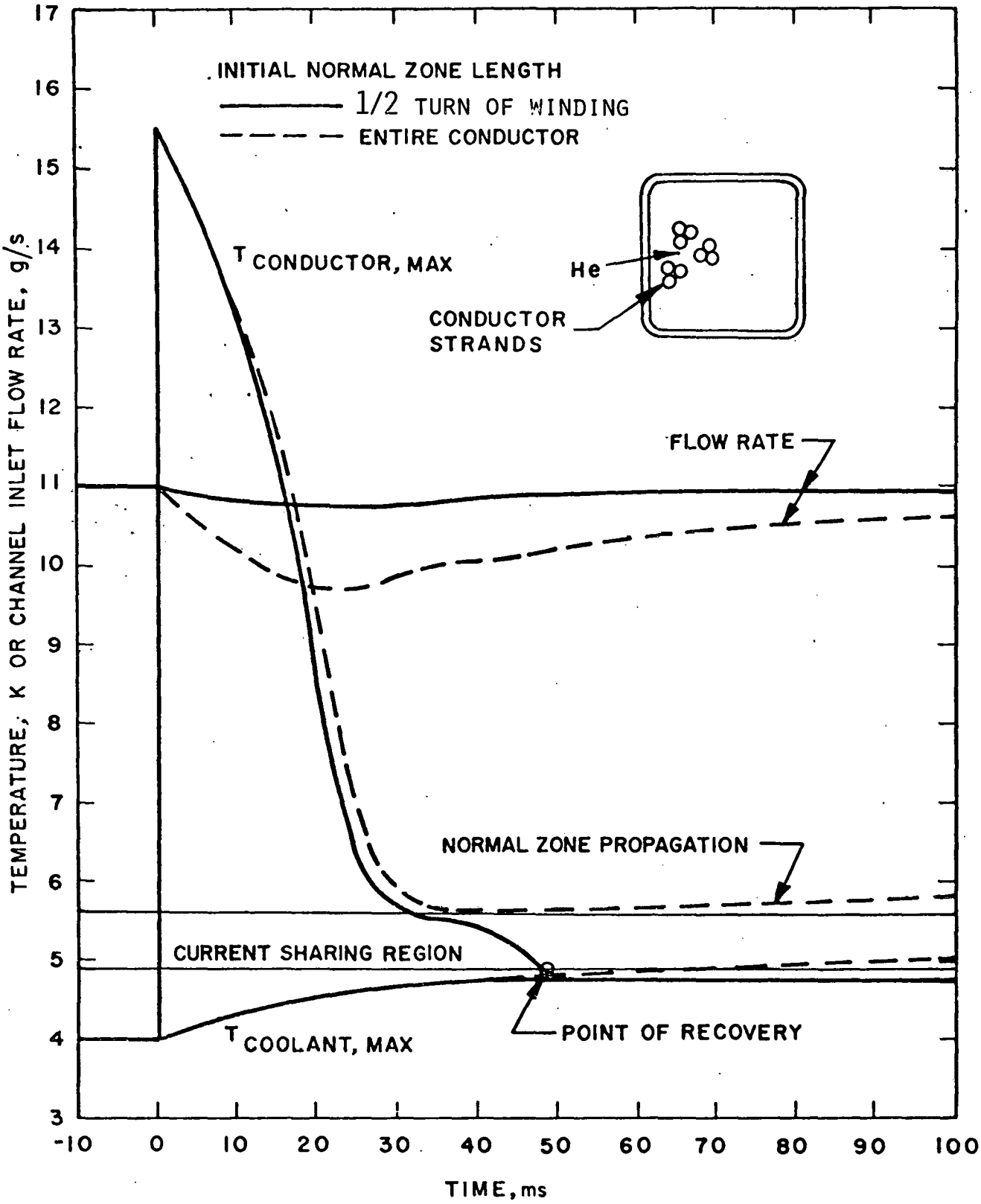

Figure 4. Temperatures and Flow Rate During Recovery Transient from an Imposed Initial Temperature of 15.5 K and Initial Inlet Flow Rate of 11 g/s for NbTi Superconductor

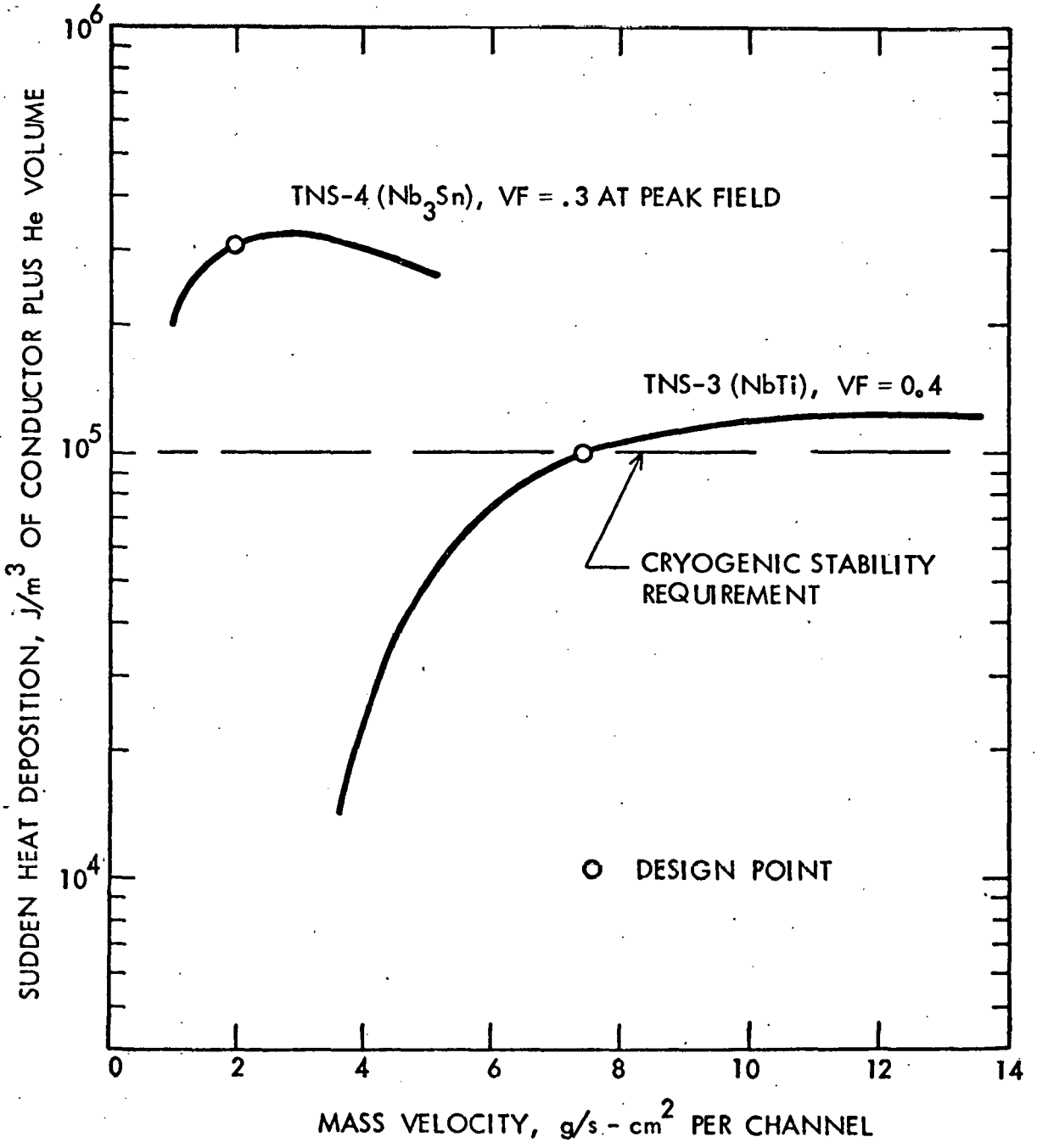

Figure 5. Recovery Capability of NbTi and Nb_3Sn Superconductors

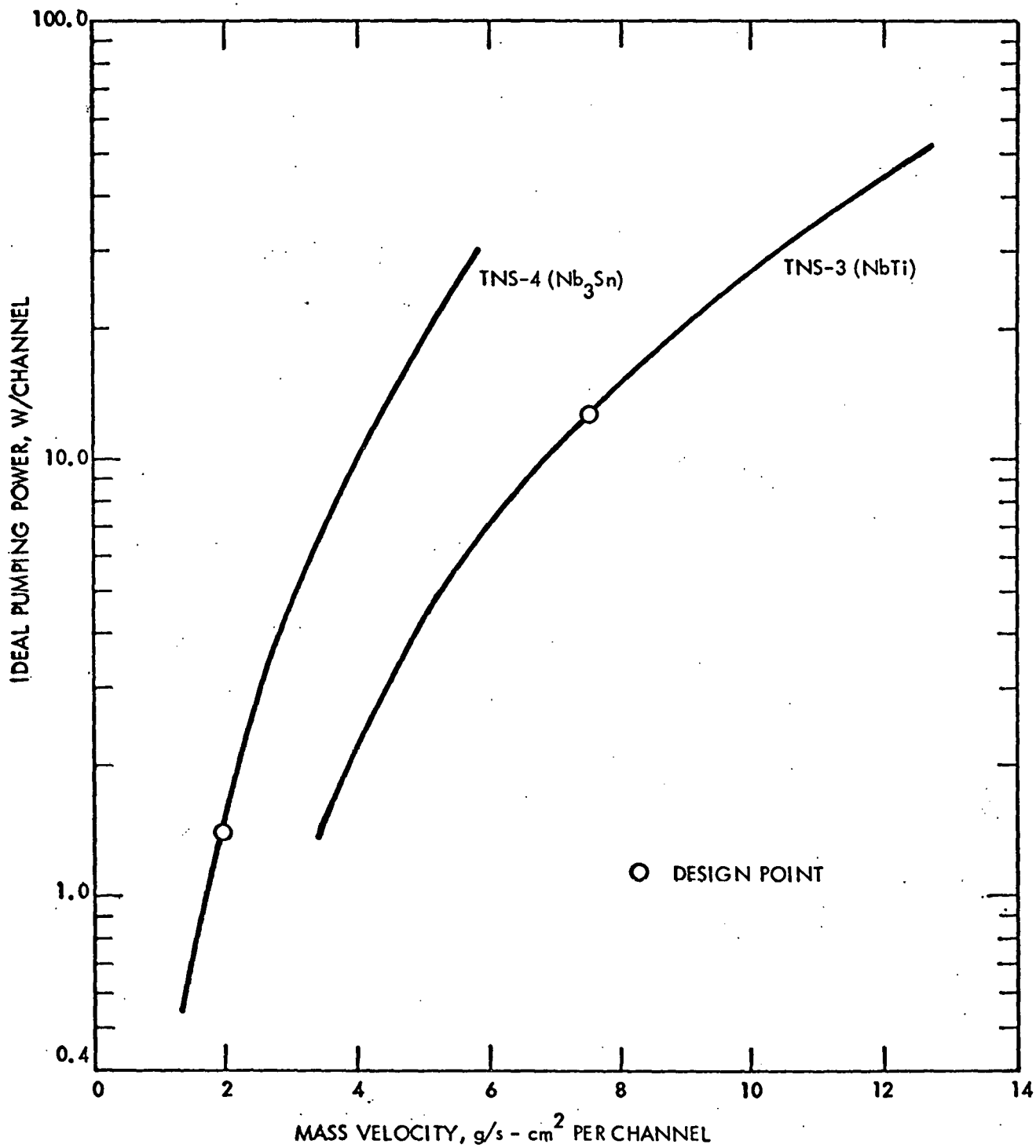

Figure 6. Ideal Pumping Power Requirements of NbTi and Nb_3Sn Superconductors.

INTERNAL DISTRIBUTION

1. Author
2. J. H. Fink
3. C. A. Flanagan
4. J. W. French
5. G. Gibson
6. D. J. Grove
7. G. W. Hardigg
8. F. M. Heck
9. J. L. Johnson
10. A. R. Jones
11. C. K. Jones
12. J. S. Karbowski
13. D. Klein
14. W. P. Kovacik
15. G. A. Krist
16. I. Liberman
17. C. J. Mole
18. R. P. Rose
19. Z. M. Shapiro
20. R. A. Smith
21. C. C. Sterrett
22. R. W. Stooksberry
23. T. C. Varljen
24. R. W. Warren
25. P. N. Wolfe
26. M. K. Wright
27. J. L. Young
28-41. Fusion Library
42-43. ARD Library

OAK RIDGE NATIONAL LABORATORY DISTRIBUTION

44. J. K. Ballou
45. J. F. Clarke
46. P. N. Haubenreich
47. M. S. Lubell
48. O. B. Morgan
49-63. M. Roberts
64. M. W. Rosenthal
65. T. E. Shannon
66. D. Steiner
67. W. C. Stoddart
68. D. W. Swain

EXTERNAL DISTRIBUTION

1. J. L. Anderson, Los Alamos Scientific Laboratory, P. O. Box 1663, Los Alamos, NM 87545.
2. D. J. Anthony, General Electric Co., Schenectady, NY 12345.
3. C. C. Baker, General Atomic Co., San Diego, CA 92138.
4. A. A. Bishop, Nuclear Engineering Programs Director, Chemical Engineering Department, University of Pittsburgh, Pittsburgh, PA 15261.
5. S. L. Bogart, Energy Research and Development Administration, Division of Magnetic Fusion Energy, Mail Stop G-234, Washington, DC 20545.
6. S. J. Buchsbaum, Bell Laboratories, Crawford Corner Road, Holmdel, NJ 07733.
7. R. W. Bussard, Energy Resources Group, Inc., 1500 Wilson Blvd., Suite 505, Arlington, VA 22209.
8. Yung-An Chao, Nuclear Science and Engineering Div., Carnegie-Mellon University, Schenley Park, Pittsburgh, PA 15213.
9. R. N. Cherdack, Burns & Roe, Inc., 283 Highway 17, Paramus, NJ 07652.
10. F. E. Coffman, Energy Research and Development Administration, Division of Magnetic Fusion Energy, Mail Stop G-234, Washington, DC 20545.
11. D. R. Cohn, Francis Bitter Laboratory, MIT, 120 Albany St., Cambridge MA 02139.
12. R. W. Conn, Nuclear Engineering Dept., University of Wisconsin, Madison, WI 53706.
13. E. C. Creutz, National Science Foundation, 1800 G Street, N.W., Washington, DC 20440.

14. H. S. Cullingford, Energy Research and Development Administration, Division of Magnetic Fusion Energy, Mail Stop G-234, Washington, DC 20545.
15. R. C. Davidson, U.S. Energy Research and Development Administration, Division of Magnetic Fusion Energy, Mail Stop G-234, Washington, DC 20545.
16. N. A. Davies, Energy Research and Development Administration, Division of Magnetic Fusion Energy, Mail Stop G-234, Washington, DC 20545.
17. S. O. Dean, Energy Research and Development Administration, Division of Magnetic Fusion Energy, Mail Stop G-234, Washington, DC 20545.
18. A. Favale, Grumman Aerospace Corp., Bethpage, NY 11714.
19. S. Fernback, Lawrence Livermore Laboratory, Livermore, CA 94551.
20. E. von Fischer, Bechtel Corp., P. O. Box 3965, San Francisco, CA 94119.
21. H. K. Forsen, Exxon Nuclear Co., 777 106th Ave. N.E., Bellevue, WA 98004.
22. T. K. Fowler, University of California, Lawrence Radiation Laboratory, P. O. Box 808, Livermore, CA 94551.
23. H. P. Furth, Princeton Plasma Physics Laboratory, Princeton University, P. O. Box 451, Princeton, NJ 08540.
24. M. B. Gottlieb, Princeton Plasma Physics Laboratory, Princeton University, P. O. Box 451, Princeton, NJ 08540.
25. W. C. Gough, Electric Power Research Institute, Palo Alto, CA 94304.
26. J. Nelson Grace, Energy Research and Development Administration, Division of Magnetic Fusion Energy, Mail Stop G-234, Washington, DC 20545.
27. R. Harder, General Atomic Co., P. O. Box 81608, San Diego, CA 92138.
28. C. D. Henning, Energy Research and Development Administration, Division of Magnetic Fusion Energy, Mail Stop G-234, Washington, DC 20545.
29. G. K. Hess, Jr., Division of Magnetic Fusion Energy, U.S. Energy Research and Development Administration, Washington, DC 20545.
30. A. G. Hill, Plasma Fusion Center, Room 4-232, Massachusetts Institute of Technology, 77 Massachusetts Avenue, Cambridge, MA 20139.
31. R. L. Hirsch, Exxon Nuclear Corp., RM. 4330, 1251 Avenue of the Americas, New York, NY 10020.
32. T. Kammash, The University of Michigan, College of Engineering, Dept. of Nuclear Engineering, Ann Arbor, MI 48109.
33. E. E. Kintner, Energy Research and Development Administration, Division of Magnetic Fusion Energy, Mail Stop G-234, Washington, DC 20545.
34. G. Kulcinski, Nuclear Engineering Dept., University of Wisconsin, Madison WI 53706.
35. D. Kummer, McDonnell Douglas, P. O. Box 516, St. Louis, MO 63166.
36. V. A. Maroni, Argonne National Laboratory, 9700 S. Cass Ave., Argonne, IL 60439.
37. D. M. Meade, Princeton Plasma Physics Laboratory, Princeton University, P. O. Box 451, Princeton, NJ 08540.
38. G. H. Miley, Nuclear Engineering Program, 214 Nuclear Engineering Laboratory, University of Illinois, Urbana, IL 61801.
39. R. Mills, Princeton Plasma Physics Laboratory, Princeton University, P. O. Box 451, Princeton, NJ 08540.
40. K. Moses, Energy Research and Development Administration, Division of Magnetic Fusion Energy, Mail Stop G-234, Washington, DC 20545.
41. M. R. Murphy, Energy Research and Development Administration, Division of Magnetic Fusion Energy, Mail Stop G-234, Washington, DC 20545.
42. S. Naymark, Nuclear Services Corp., 1700 Dell Ave., Campbell, CA 95008.
43. J. O. Neff, Energy Research and Development Administration, Division of Magnetic Fusion Energy, Mail Stop G-234, Washington, DC 20545.
44. T. Ohkawa, General Atomic Co., P. O. Box 608, San Diego, CA 92112.
45. J. Powell, Brookhaven National Laboratory, Upton, Long Island, NY 11973.
46. J. R. Purcell, General Atomic Co., P. O. Box 608, San Diego, CA 92112.

47. P. J. Reardon, Princeton Plasma Physics Laboratory, Princeton University, P. O. Box 451, Princeton, NJ 08540.
48. D. J. Rose, Department of Nuclear Engineering, Massachusetts Institute of Technology, Cambridge, MA 02139.
49. P. Sager, General Atomic Co., P. O. Box 608, San Diego, CA 92112.
50. G. A. Sawyer, Los Alamos Scientific Laboratory, P. O. Box 1663, Los Alamos, NM 87545.
51. L. C. Schmid, Pacific Northwest Laboratories, Battelle Blvd., P. O. Box 999, Richland, WA 99352.
52. M. A. Schultz, Nuclear Engineering Department, The Pennsylvania State University, 231 Sackett Building, University Park, PA 16802.
53. Weston M. Stacey, Jr., Georgia Institute of Technology, Atlanta, GA 30332.
54. C. M. Stickley, Division of Laser Fusion, U.S. Energy Research and Development Administration, Washington, DC 20545.
55. C. E. Taylor, Lawrence Livermore Laboratory, Mail Code L-384, P. O. Box 808, Livermore, CA 94550.
56. V. Teofilo, Pacific Northwest Laboratories, Battelle Blvd., P. O. Box 999, Richland, WA 99352.
57. K. Thomassen, Lawrence Livermore Laboratory, P. O. Box 808, Livermore, CA 94550.
58. B. Twining, Energy Research and Development Administration, Division of Magnetic Fusion Energy, Mail Stop G-234, Washington, DC 20545.
59. A. W. Trivelpiece, Engineering and Research, Maxwell Laboratories, Inc., 9244 Balboa Avenue, San Diego, CA 92123.
60. J. M. Williams, Energy Research and Development Administration, Division of Magnetic Fusion Energy, Mail Stop G-234, Washington, DC 20545.
61. H. H. Woodson, Department of Electrical Engineering, University of Texas, Austin, TX 78712.
62. H. Yoshikawa, Westinghouse Hanford Co., P. O. Box 1970, Richland, WA 99352.
63. K. Zwilski, Energy Research and Development Administration, Division of Magnetic Fusion Energy, Mail Stop G-234, Washington, DC 20545.
64. Energy Research and Development Administration, Technical Information Center, P. O. Box 62, Oak Ridge, Tennessee 37830.